Protein Science (2000), *9*:544–551. Cambridge University Press. Printed in the USA.
Copyright © 2000 The Protein Society

The X-ray structure of a chitinase from the pathogenic fungus *Coccidioides immitis*

THOMAS HOLLIS,[1] ARTHUR F. MONZINGO,[1] KARA BORTONE,[1] STEPHEN ERNST,[1] REBECCA COX,[2] AND JON D. ROBERTUS[1]

[1]Institute of Cellular and Molecular Biology, Department of Chemistry and Biochemistry, University of Texas, Austin, Texas 78712
[2]Department of Clinical Investigation, Texas Center for Infectious Disease, San Antonio, Texas 78223

(RECEIVED November 10, 1999; FINAL REVISION December 13, 1999; ACCEPTED January 7, 2000)

Abstract

The X-ray structure of chitinase from the fungal pathogen *Coccidioides immitis* has been solved to 2.2 Å resolution. Like other members of the class 18 hydrolase family, this 427 residue protein is an eight-stranded β/α-barrel. Although lacking an N-terminal chitin anchoring domain, the enzyme closely resembles the chitinase from *Serratia marcescens*. Among the conserved features are three *cis* peptide bonds, all involving conserved active site residues. The active site is formed from conserved residues such as tryptophans 47, 131, 315, 378, tyrosines 239 and 293, and arginines 52 and 295. Glu171 is the catalytic acid in the hydrolytic mechanism; it was mutated to a Gln, and activity was abolished. Allosamidin is a substrate analog that strongly inhibits the class 18 enzymes. Its binding to the chitinase hevamine has been observed, and we used conserved structural features of the two enzymes to predict the inhibitors binding to the fungal enzyme.

Keywords: beta-alpha barrel; chitinase; fungal pathogen; mutagenesis; X-ray structure

Fungal infections constitute a major problem in human pathogenesis. These run from relatively benign but stubborn skin infections like ring worm, to life-threatening lung infections like coccidioidomycosis (San Joaquin Valley fever) caused by *Coccidioides immitis* (Cole & Kirkland, 1991). Fungal infections can be particularly dangerous in immuno-compromised patients, like those with HIV infections. The severity of such fungal infections, particularly from *Candida*, *Coccidioides*, *Cryptococcus*, and *Histoplasmosis*, has been extensively reviewed (Ampel, 1996; Minamoto & Rosenberg, 1997).

Chitin is an insoluble β-1,4-linked polymer of N-acetylglucosamine (NAG) vital to fungal cell wall integrity. Mutations that inactivate chitin synthase genes can lead to a loss of fungal viability (Bulawa & Osmond, 1990). In addition to chitin synthases, fungi code for several chitinases that are also required for cell growth (Kuranda & Robbins, 1991). In essence, fungi need chitinases to disrupt existing cell walls as part of normal cell division. Because chitin is not a component of mammalian cells, this difference is potentially exploitable in the design of specific antifungal agents. Presently, the best-known inhibitor is the antibiotic allosamidin, a glycoside derived from *Streptomyces* (Nishimoto et al., 1991); it inhibits *Candida* chitinase with a K_i of 5 μM (Milewski et al., 1992).

Coccidioides immitis is the causative agent of coccidioidomycosis (San Joaquin Valley fever), one the of the most widespread endemic diseases in America. Diagnosis of the disease and monitoring of its prognosis has been carried out largely through the development of serologic tests (Pappagianis & Zimmer, 1990). The primary *Coccidioides* antigen was identified as a chitinase (Johnson & Pappagianis, 1992), and a specific monoclonal antibody has been raised against it (Dolan & Cox, 1991). Molecular cloning revealed that the fungus expresses two chitinases, called CTS1 and CTS2 (Pishko et al., 1995). Cloning of the gene for the principle *Coccidioides* complement fixing antigen revealed it to be identical with CTS1, and it was described as the CF/chitinase protein (Yang et al., 1996). For this paper, we will refer to the *Coccidioides immitis* chitinase-1 molecule as CiX1.

CiX1 is a 427 residue protein that is found both in the cytoplasm and expressed on the cell surface—consistent with its antigenicity. Based on amino acid sequence similarities, the enzyme is a member of glycohydrolase family 18, together with chitinases from other fungi, as well as bacteria and a few plants (Henrissat & Bairoch, 1993). The similarity among members of this family is illustrated in Figure 1. It compares the CiX1 amino acid sequences with two other fungal chitinases, *Trichoderma harzianum* (Garcia et al., 1994) and *Aphanocladium album* (Blaiseau & Lafay, 1992), and a bacteria chitinase from *Serratia marcescens* (Perrakis et al., 1994). The similarity among the fungal enzymes is strong, exhibiting roughly 50% sequence identity. The bacterial enzyme sequence is about 25% identical with the fungal enzymes. It is clear that these enzymes are homologs, although the bacterial enzyme has a 120-residue amino terminal domain, not found on the fungal enzymes, which is thought to act as a chitin binding anchor. The

Reprint requests to: Jon Robertus, Institute of Cellular and Molecular Biology, Department of Chemistry and Biochemistry, University of Texas, Austin, Texas 78712; e-mail: jrobertus@mail.utexas.edu.

```
                10        20        30        40        50        60
Chi-ci   MRFLIGALLTLQTLVQASSMSSMPNYYPVPEAPAEGGFRSVVYFVNWAIYGRGHNPQDLK
Chi-th   MLSFLGKSVALLAALQATLSSPKPGHRRASVEKRANGYANSVYFTNWGIYDRNFQPADLV
Chi-aa   MLSFVKKSIALVAALQAVTALATPISSEAGVEKRGSGFANAVYFTNWGIYGRNFQPADLP
Chi-sm   TASDATEIVVADTDGSHLAPLKEPLLEKNKPYKQNSGKVVGSYFVEWGVYGRNFTVDKIP

             70                                        80        90
Chi-ci   ADQFTHILYAFANIRP-------------------------SGEVYLSDTWADTDK-HY
Chi-th   ASDVTHVIYSFMNLQA-------------------------DGTVISGDTYADYEK-HY
Chi-aa   ASEITHVLYSFMNVRA-------------------------DGTIFSGDTYADYEK-HY
Chi-sm   AQNLTHLLYGFIPICGGNGINDSLKEIEGSFQALQRSCQGREDFKVSIHDPFAALQKAQK

         100       110       120       130       140       150
Chi-ci   PGDKWDEPGNNVYGCIKQMYLLKKNNRNLKTLLSIGGWTYSPNFKTPASTEEGRKKFADT
Chi-th   ADDSWNDVGTNAYGCVKQLFKVKKANRGLKVLLSIGGWTWSTNFPSAASTDANRKNFAKT
Chi-aa   AGDSWNDVGTNAYGCVKQLYLLKKQNRNMKVMLSIGGWTWSTNFPAAASSAATRKTFAQS
Chi-sm   GVTAWDDPYKGNFG---QLMALKQAHPDLKILPSIGGWTLSDPF-FFMGDKVKRDRFVGS

         160       170                 180       190       200
Chi-ci   SLKLMKDLG-FDGIDIDWEYPE---------DEKQANDFVLLLKACREALDAYSANHPNG
Chi-th   AITFMKDWG-FDGIDIDWEYPA---------DATQASNMILLLKEVRSQRDAYAAQYAPG
Chi-aa   AVGFMKDWG-FDGIDIDWEYPA---------DATQAQNMVLLLQAVRSELDSYAAQYAKG
Chi-sm   VKEFLQTWKFFDGVDIDWEFPGGKGANPNLGSPQDGETYVLLMKELRAMLDQLSAE--TG

         210       220       230       240       250       260
Chi-ci   KKFLLTIASPAGPQNYNKLKLAEMDKYLDFWNLMAYDFSGSWD-KVSGHMSNVFPSTTKP
Chi-th   YHFLLTIAAPAGKDNYSKLRLADLGQVLDYINLMAYDYAGSFS-PLTGHDANLFNNPSNP
Chi-aa   HHFLLSIAAPAGPDNYNKLKFAELGKVLDYINLMAYDYAGSWS-NYTGHDANIYANPQNP
Chi-sm   RKYELTSAISAGKDKIDKVAYNVAQNSMDHIFLMSYDFYGAFDLKNLGHQTALNAPAWKP

             270       280       290       300             310
Chi-ci   ESTPFSSDKAVKDYIKAGVPANKIVLGMPLYGRAFASTDG------IGTSFNGVGGGSWE
Chi-th   NATPFNTDSAVKDYINGGVPANKIVLGMPIYGRSFQNTAG------IGQTYNGVGSGSWE
Chi-aa   NATPYNTDDAVQAYINGGVPANKIVLGMPIYGRSFQQTEG------IGKPYNGIGSGSWE
Chi-sm   D-TAYTTVNGVNALLAQGVKPGKVVVGTAMYGRGWTGVNGYQNNIPFTGTATGPVKGTWK

          320           330       340       350       360       370
Chi-ci   NGVWDYKDMP----QQGAQVTELEDIAASYSYDKNKRYLISYDTVKIAGKKAEYITKNGM
Chi-th   AGIWDYKALP----KAGATVQYDSVAKGYYSYNSATKELISFDTPDMINTKVAYLKSLGL
Chi-aa   NGIWDYKALP----KAGATVKCDDTAKGCYSYDPSTKELISFDTPAMISTKVSWLKGKGL
Chi-sm   NGIVDYRQIAGQFMSGEWQYTYDATAEAPYVFKPSTGDLITFDDARSVQAKGKYVLDKQL

             380       390       400       410       420
Chi-ci   GGGMWWESSSDKTGNESLVGTVVNGLGGTGKLEQRENELSYPESVYDNLKNGMPS
Chi-th   GGSMFWEASADKKGADSVIGTSHRALGG---LDTTQNLLSYPNSKYDNIKNGLN
Chi-aa   GGTMFWEASASKKGSDSLISTSHQGLGS---QDSTQNYLDYPNSKYDNIKKGMN
Chi-sm   GGLFSWEIDADN---GDILNSMNASLGNSAGVQ----------------------
```

Fig. 1. Comparison of class 18 chitinase primary structures. The sequences correspond to *C. immitis*, *T. harzianum*, *A. album*, and *S. marcescens*, respectively. The numbering corresponds to the *C. immitis* sequence. All sequences begin at residue 1 except *S. marcescens*, which begins at 121. Invariant residues are shown in bold.

X-ray structure for the *Serratia* chitinase has been solved (Perrakis et al., 1994). It shows the chitinase enzyme is an eight stranded β/α-barrel, $(\beta\alpha)_8$, while the N-terminal domain is a discrete unit with a β-sandwich configuration. The class 18 chitinases differ in sequence and structure from the class 19 chitinases, like those from many higher plants (Hart et al., 1995) that have a structural relationship to lyzozymes (Monzingo et al., 1996).

Hevamine is a plant chitinase, from family 18, which is more distantly related to the fungal enzymes. The 273 residue protein is substantially smaller than CiX1 and shows only 14% sequence identity with it. The X-ray structure for hevamine has been solved (Terwisscha van Scheltinga et al., 1996) and also exhibits $(\beta\alpha)_8$ structure. Hevamine has been complexed with allosamidin, and analysis of the structure led to the notion that the mechanism of cleavage for chitin may proceed by anchimeric assistance through an oxazoline intermediate (Terwisscha van Scheltinga et al., 1995).

In this paper, we describe the high resolution molecular structure of the CiX1 enzyme. This is the first structure of a chitinase from a fungal source and should serve as the archetype for a variety of related enzymes, many of which may be targets for antifungal inhibitor design. A model is proposed for binding the substrate analog allosamidin.

Results and discussion

Amino terminus characterization

Edman sequencing of purified CiX1 revealed that the amino terminal residues were Tyr-Pro-Val-Pro-Glu-Ala-Pro-Ala-Glu-Gly-Gly-Phe-Arg-Ser-Val. This corresponds to residues 27–41 of the chitinase gene sequence (Yang et al., 1996).

Structure determination

X-ray diffraction data were collected to 2.2 Å resolution (99.7% complete) on the native CiX1 crystals and to 2.5 Å on a *p*-hydroxymercuribenzoate (PHMB) derivative. The data collection information is summarized in Table 1. Difference Patterson analysis of the PHMB derivative revealed a single mercury site with modest phasing power.

We also used molecular replacement (MR) methods to phase the CiX1 data. The refinement of the CiX1 model was carried out in 22 rounds, as described in Materials and methods. After the final round of refinement, a total of 392 amino acid residues had been fit corresponding to sequence numbers 36 through 427. Residues 27 to 35, identified by Edman sequencing, are apparently in thermal motion and could not be seen in the density maps or positioned in the model. In addition, 241 water molecules with discrete electron density and in position to hydrogen bond to polar protein atoms were added to the model. The final model working *R*-factor was 17.6%, and the free *R* was 25.8%. The RMS bond deviation of the model from ideality is 0.007 Å, and the deviation in bond angles is 1.36°. The Ramachandran plot has 91% of residues in the most favorable region, 8.1% in additional allowed space, 0.9% in generously allowed space, and none in the disallowed space. There are four *cis* peptide bonds at Phe71, Tyr172, Pro326, and Glu379. Figure 2 shows a $2F_o - F_c$ electron density map for a region of the final CiX1 model.

Structure description

Figure 3 shows a backbone trace of CiX1 viewed down the axis of the barrel. Figure 4 is a representation of the secondary structure arrangement and nomenclature used in this description. The eight parallel β-strands that form the core of the enzyme are labeled S1 to S8. As in all $(\beta\alpha)_8$ barrels, strand 8 is hydrogen bonded to strand 1. In general, β/α-barrel structures are such that a given β-strand is followed by an α-helix "return stroke." There is no α-helix on the return between β-strands 1 and 2, and as a result, no

Table 1. *Data collection statistics for CiX1*

	Native	PHMB
Resolution (Å)	2.2	2.5
R_{merge} (%)	12.2	15.6
R_{merge} (last shell) (%)	21.3	39.2
I/σ_I	10.3	7.1
I/σ_I (last shell)	5.19	4.76
Unique reflections	20,899	14,669
Redundancy	6.0	5.5
Completeness (%)	99.7	99.7

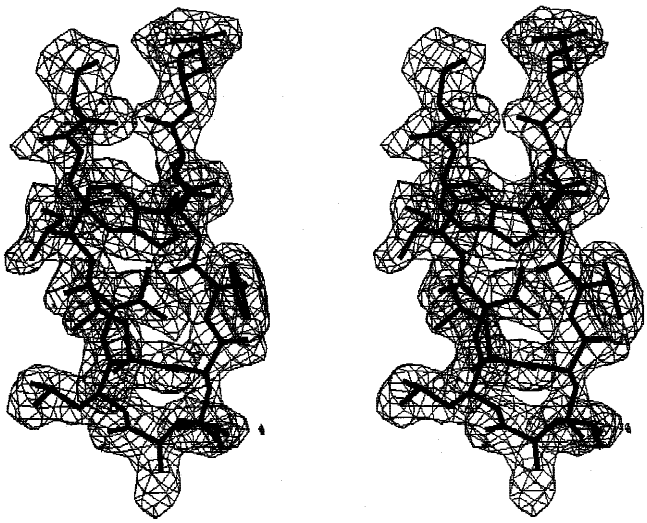

Fig. 2. Electron density map for a section of the final CiX1 model. The map is an LBEST-weighted $2F_o - F_c$ map contoured at the 1.0σ level. The superimposed model is part of the β-barrel, strands 5 and 6. The strand on the left shows residues 207 to 212, which is at the top. The right-hand strand includes residues 231 to 236, which is at the top.

helix has been labeled as 1. However, residues 45–65 have some helical character and contain at least three short 3_{10} helical loops. For example, the carbonyl oxygen of Val45 receives a hydrogen bond from the amido nitrogen of Ala48, and residues 46 and 47 bond with 49 and 50, respectively. O_{55} is bonded to N_{58} in a second 3_{10} loop, and O_{60} bonds with N_{63} in a third.

There are two α-helices following strand 2, and these are labeled H2a and H2b. These two helices appear to stack and resemble a continuous helix with a bulge looped out. To illustrate this stacking, it should be noted that O_{87} and O_{88} from the top of H2a form α-helix-like interactions with the bottom of H2b, receiving hydrogen bonds from N_{108} and N_{109}, respectively. β-Strands S3 through S8 are each followed by return helices labeled H3 through H8, respectively. A short helix near the carboxy terminus of CiX1 is labeled H9.

In addition to the β-sheet of the core, β-structure is formed within several connecting loops of the barrel. The connection between S2 and H2 contains an antiparallel two-stranded sheet labeled S2a and S2b. The connection between barrel strand S7 and H7 contains a more elaborate and structurally distinct domain in the form of a modified Greek key. As shown in Figure 4, this domain contains five β-strands labeled S7a through S7e. Table 2 identifies the amino acid residues of the various secondary structural elements in the protein.

Comparison of CiX1 and SmX

The amino acid sequence of CiX1 is about 25% identical to that of the C-terminal domain of SmX. Figure 5 shows a least-squares superposition of CiX1 (thick line) and SmX (thin line); the RMS distance between 353 equivalent Cα atoms is 1.8 Å. SmX has a distinct N-terminal β-sandwich domain, thought to serve as a chitin anchor, that is missing in CiX1. This domain is about 140 amino acids in length. SmX residues 141 through 158 act as a flexible linker joining the N-terminal domain to the catalytic β-barrel domain. This region is shown as a thin black line in Figure 5 and is marked by labels SmX24 to mark the N-terminus and SmX145, conveniently displayed near the C-terminal region of this unique domain. Val159 of SmX begins the formal hydrogen bonding pattern for the first sheet of the core. CiX1 lacks the amino terminal domain, and its amino terminus corresponds to a leader sequence and is probably processed away during maturation (Yang et al., 1996). The exact cleavage site is unknown, but our clone expresses residues 27 to 427. Residues 27–35 cannot be seen, but Gly36 is visible and leads to S1, which formally begins with residue 39. Arg39 of CiX1 superimposes with Val159 of SmX and can be said to define the beginning of the structurally conserved catalytic core domain.

As seen in Figure 5, the two core domains are generally superimposable over the majority of the $(\beta\alpha)_8$ barrel. Figure 1 shows there are a few multiresidue differences between the proteins. SmX has four insertions of note, and their locations are labeled in Figure 5. These include a 26 residue insertion in the loops between S2a and S2b, a nine-residue insertion between S4 and H4, a six-residue insertion between S7a and S7b, and four-residue insertion in the loop between S7b and S7c. The first two insertions interact with one another and contribute to one wall of the active site cleft. Because no substrate analogs have been complexed to CiX1 or to SmX, we cannot state that the insertion plays no role in substrate binding. However, its position is far from the likely catalytic site, and it seems unlikely that the insertions effect enzyme activity in any important way. The other insertions appear to have no functional consequence either. CiX1 has a slightly elongated C-terminal tail compared with SmX, which lies on the bottom of the molecule far from the active site; this tail is shown as a thick gray line in Figure 5.

CiX1, like most class 18 glycohydrolases, contains a number of cis peptide bonds. One involves a *cis* Pro, that is, the bond between Met325 and Pro326. In addition, there are three non-Pro *cis* bonds. These are between Ala70 and Phe71, Glu171 and Tyr172, and Trp378 and Glu379. All three of these *cis* bonds are conserved in SmX (Perrakis et al., 1994), and the first and third bonds are conserved in hevamine (Terwisscha van Scheltinga et al., 1996). It is important to note that the residues involved in the three non-proline *cis* bonds all play an important part in the architecture of the catalytic site of CiX1.

The CiX1 active site

Proteins belonging to the class 18 family of chitinases have two signature sequences, as seen in Figure 1 corresponding to CiX1 residues 127–132 and 163–173. These residues lie along barrel strands 3 and 4 of the class 18 chitinases (Terwisscha van Scheltinga et al., 1996) and help form the active site cleft on the carboxyl end of the β-barrel. The clustering of these and other conserved residues make the active site cleft of CiX1 easy to identify. To aid in the structural analysis, we wanted to position the substrate analog allosamidin, seen crystallographically in the plant chitinase hevamine (Terwisscha van Scheltinga et al., 1995), into the CiX1 active site. Although there is only 14% amino acid identity between CiX1 and hevamine, the two proteins are homologous and can be superimposed in a least-squares sense with an RMS distance of 2.9 Å between 205 equivalent Cα atoms. The position of allosamidin with respect to the overall enzyme structure is indicated in Figure 3A, the ribbon representation of CiX1.

Figure 6 shows the binding of allosamidin in more detail. The inhibitor is represented by the thickest bonds. Key residues from

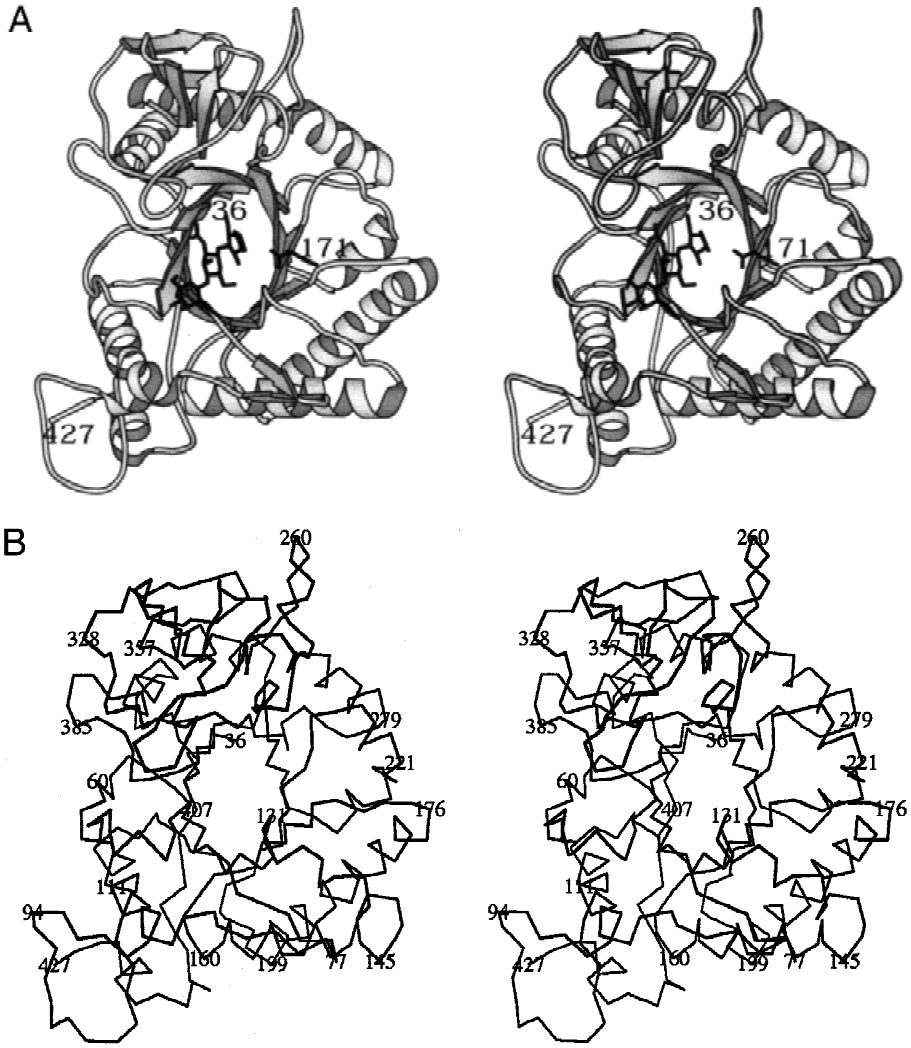

Fig. 3. The backbone trace of CiX1. **A:** A ribbon drawing of the enzyme. The position of allosamidin is shown in heavy black bonds, and the position of the Glu171 side chain is also indicated. **B:** A Cα trace of CiX1, with marker residues labeled by their amino acid sequence number.

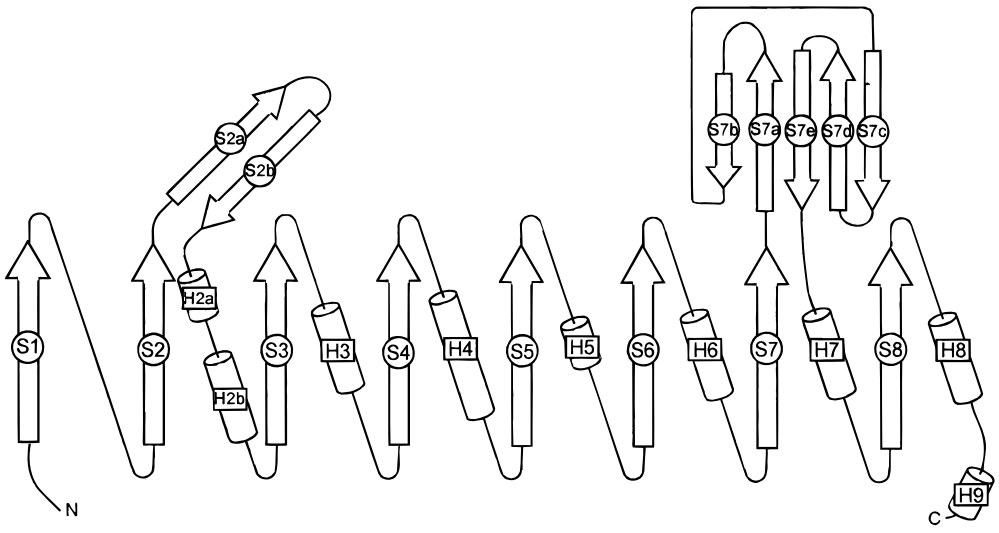

Fig. 4. A cartoon representation of CiX1 secondary structural elements.

Table 2. *CiX1 secondary structure*

β-Strand	Residues	α-Helix	Residues
S1	39–46	H2a	84–91
S2	65–70	H2b	107–119
S3	123–128	H3	143–161
S4	165–170	H4	175–199
S5	207–212	H5	223–230
S6	232–239	H6	268–280
S7	285–292	H7	356–371
S8	373–379	H8	389–399
		H9	418–425
S2a	73–75		
S2b	78–81		
S7a	295–300		
S7b	318–320		
S7c	331–335		
S7d	340–346		
S7e	349–354		

hevamine are shown as the thinnest bonds, while their homologs from CiX1 are intermediate. The labels correspond to CiX1 residues. The oxazolium ring (suspected transition state analog) rests on Trp378 (Trp255 in hevamine). Glu171 (hevamine 127) is the catalytic acid and is poised near the scissile bond of a polysaccharide substrate, which would continue off to the upper left in the figure. Asp169 is the analog of hevamine 125, which may form an ion pair with the positively charged nitrogen of the oxazolium ring. In CiX1, the carboxylate is rotated away to hydrogen bond to Tyr43; presumably in a real complex, it would rotate to a position similar to that seen in the hevamine complex. Asp240 (hevamine Asn184) and Tyr239 (hevamine 183) can make hydrogen bonds with the substrate analog, while Tyr43 (hevamine 6) and Phe71 (hevamine 32) contribute to the active site geometry. The interactions with sugars at the nonreducing end of the substrate differ in detail between the two enzymes. For example Trp47, shown in dashed bonds, is invariant in the larger class 18 hydrolases (Fig. 1) and appears to serve as a platform to bind these sugars. The corresponding residue in hevamine is Gln9, which binds to the N-acetyl group of the last sugar ring (Terwisscha van Scheltinga et al., 1995). In addition to Trp47, specifically illustrated in Figure 6, there are several other residues, conserved in the CiX1 homologs, that are in a position to interact with the substrate. These include Arg52, Trp131, Thr132, Arg295, Trp315, Tyr293, and Asp321.

The side-chain positions in Figure 6 are those seen in the CiX1 apoprotein X-ray structure, and the allosamidin position is based solely on the mathematical operator relating the Cα positions of residues conserved between the CiX1 and hevamine barrels. No effort has been made to refine the inhibitor complex using energy functions or other methods to optimize protein–ligand interactions. We suspect that the CiX1 conformation does change upon allosamidin binding because all our efforts to soak the inhibitor into CiX1 crystals resulted in cracking. Nevertheless, this docking experiment is very likely to indicate those amino acid groups that participate in binding the substrate analog, especially near the cleavage site.

As mentioned, Glu171 is near the position in the active site cleft that would be occupied by the susceptible glycosidic bond of a natural substrate. The class 18 chitinases are known to act through a mechanism that retains the anomeric configuration of the product (Armand et al., 1994). Such retaining enzymes are often thought to act through a double displacement mechanism, like hen lysozyme (Blake et al., 1967). This mechanism requires two catalytic groups,

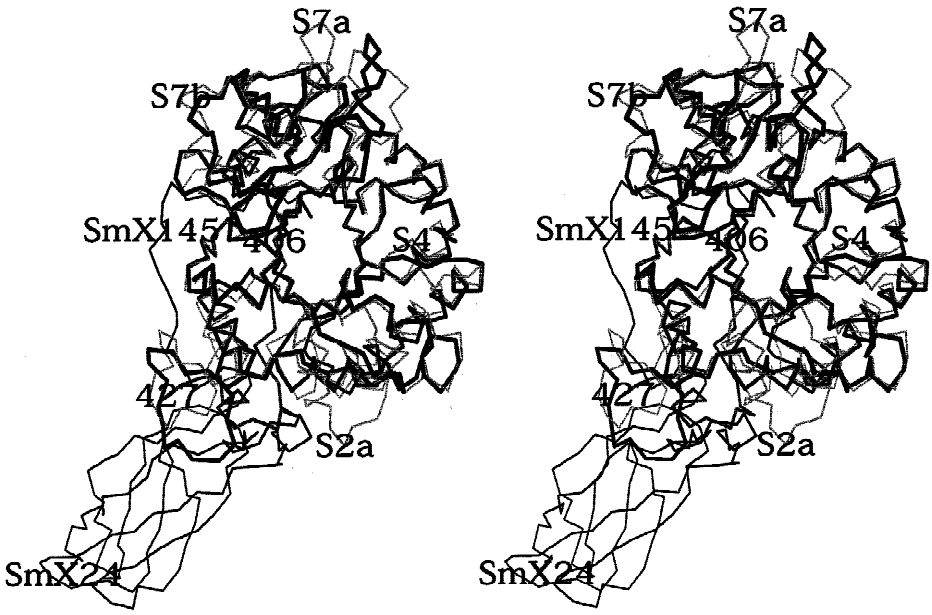

Fig. 5. A superposition of CiX1 and SmX. CiX1 is traced in thick bonds, while SmX is in thin bonds. SmX has a 120 residue chitin anchoring domain, shown at lower left as a thin black line, which is absent in the CiX1 molecule. The remainder of the chain is a thin gray line. The C-terminal residues of CiX1, 406–427, are missing in SmX, and are shown as a thick gray line.

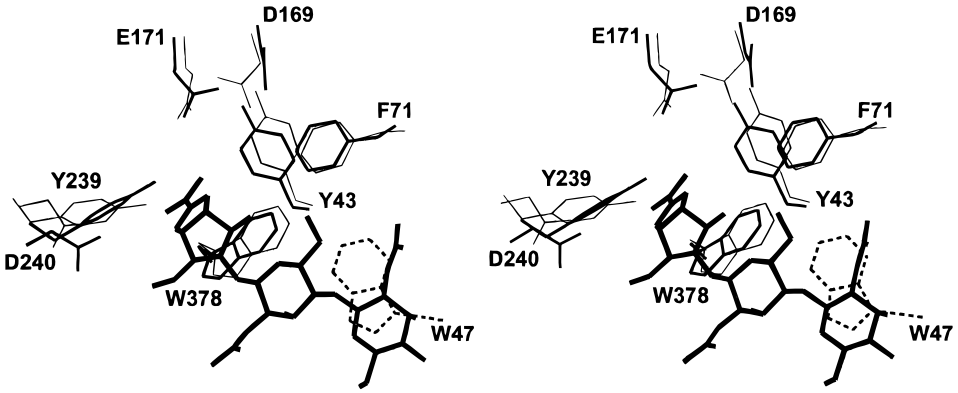

Fig. 6. A model of allosamidin and conserved residues from the CiX1 active site. Allosamidin is shown in the thickest bonds, CiX1 side chains are shown as intermediate bonds, and their hevamine homologs are the thin bonds. The labels correspond to CiX1 residues.

an acid to protonate the leaving group, and a carboxylate to stabilize a suspected oxycarbonium intermediate. The acid group is thought to be Glu171 in CiX1. Site-directed mutagenesis of a bacterial class 18 chitinase shows that the homologous residue is crucial to enzyme activity (Watanabe et al., 1993). Because no second mechanistic group could be identified in the hevamine structure, it was hypothesized that class 18 enzymes do operate by double displacement but use a mechanism that involves anchimeric assistance. That is, during catalysis the carbonyl oxygen of the C2 N-acetyl group forms a bond to C1 forming an oxazoline intermediate (Terwisscha van Scheltinga et al., 1995). This mechanism is supported by molecular mechanics calculations (Brameld et al., 1998). The oxazoline group of allosamidin is thought to mimic the transition state of the proposed hydrolytic reaction (Terwisscha van Scheltinga et al., 1995), which would account for its tight binding.

The structure of CiX1 and the model of allosamidin binding shown in Figure 6 are consistent with the conservation of the signature sequences and the proposed roles for many of these residues. The first signature sequence appears to interact directly with the substrate where Trp131 contacts the oxazoline group. Thr132 is in position to form a hydrogen bond with the C6 hydroxyl of the N-acetyl glucosamine in the middle of the inhibitor. The second signature sequence does not appear to make many direct contacts with the substrate but does provide the suspected catalytic acid, Glu171. The oxazoline ring interacts with the side chains of Phe71, Glu171, and Trp378, all residues that are involved in *cis* peptides. Presumably these residues are crucial to preserving the correct peptide geometry for binding and catalysis.

Analysis of the E171Q mutant

To confirm that Glu171 of CiX1 is indeed a key active site residue, we used site-directed mutagenesis to convert it to a glutamine (E171Q). We used the hydrolysis of 4-methylumbelliferyl β-*N*,*N*′,*N*″-triacetylchitotrioside, which releases a fluorescent product, to measure chitinase activity (Hollis et al., 1997). The data, not shown, indicated that conversion of Glu171 to the neutral amide completely inactivating the enzyme, in agreement with mutagenic data for a bacterial enzyme (Watanabe et al., 1993). This strengthens the notion that both the overall structure and also the mechanism are conserved between fungal and bacterial representatives of the class 18 enzymes.

Conclusions

Fungal infections are a major health issue, and the development of antifungal agents is an area of intense research. Enzymes involved in fungal cell wall metabolism, including chitinases, are a logical target for inhibitor design. We have solved the X-ray structure of the first fungal chitinase. It is likely that the chitinase from *C. immitis* is a good model for the enzyme from other fungal species. The inhibitor allosamidin has been observed in the plant chitinase hevamine complex. We made an analogous model for binding this substrate analog into the fungal enzyme. It suggests that the active site is formed only by residues conserved in the fungal enzyme family. Glu171, by analogy to other class 18 glycohydrolases, is thought to be the catalytic acid. Site-directed mutagenesis, converting the amino acid to Gln, eliminates any detectable enzyme activity, consistent with this hypothesis.

Materials and methods

Crystal structure determination

CiX1 was expressed as a fusion with glutathione S transferase as described earlier (Hollis et al., 1998). Purified CiX1 was subjected to automated N-terminal Edman sequencing at the Protein Sequencing Center at the University of Texas. The crystallization of *C. immitis* chitinase and the data collection of the native and *p*-hydroxymercuribenzoate (PHMB) data sets, using an RAXIS IV detector on a Rigaku RU-200 generator with double-focusing mirrors, have been described previously (Hollis et al., 1998).

The primary amino acid sequence of CiX1 (Yang et al., 1996) was aligned with that of the *Serratia marcesans* chitinase, SmX (Jones et al., 1986), using CLUSTAL V (Higgins et al., 1992). The following models based on the SmX crystal structure (Protein Data Bank (PDB) entry 1CTN) (Perrakis et al., 1994) were used: (1) residues 158–558 of the SmX structure with loop 195–220 and several smaller loops deleted (abbreviated SmX′), (2) SmX′ with the CiX1 sequence substituted, (3) SmX′ with alanine substituted for all residues, and (4) SmX′ with alanine substituted for all residues except conserved hydrophobic residues. Rotation and translation searches and Patterson correlation refinement (Brünger, 1990) were done with the four models using X-PLOR (Brünger, 1992). For all four models, the 80 or so highest peaks from the rotation function were analyzed to determine their Patterson correlation.

The best Patterson correlation for the three models of SmX′ with substituted sequences corresponded to the same rotation angles. The refined Patterson correlation for these models was 0.04, 30–39% higher than next best correlation. The best Patterson correlation for the unsubstituted SmX′ model corresponded to a different set of rotation angles, and it had a lower correlation value of 0.03.

Using the rotational orientation that yielded the best Patterson correlation with the three sequence-substituted models, translation searches were done in both enantiomorphic space groups $P4_12_12$ and $P4_32_12$. All three models gave the same highest translation function peak of five to seven standard deviations above the mean with the $P4_12_12$ search. In the $P4_32_12$ search, all three models gave the same highest translation function peak of 10–11 standard deviations above the mean. The *R*-factor for the best translation solution in $P4_32_12$ for the CiX1 sequence-substituted model was 0.52. A difference Fourier of the PHMB derivative data using phases from the translated CiX1 sequence model returned an eight standard deviation peak, which corresponded to the known Hg site. The site was within 4 Å of the Cα position of Cys108.

This initial model, which consisted of residues 40–399 (360 residues), was refined using the slow cooling protocol of X-PLOR (Brünger, 1992). The refined model had a working *R*-factor of 0.35 and an R_{free} of 0.50 (5–3.0 Å). To facilitate manual rebuilding of the model, a difference map and a $2F_o - F_c$ map, weighted to eliminate bias from the model, were prepared. A difference map of the form $(F_o - F_c)\alpha_{calc}$ was calculated using X-PLOR. To prepare the unbiased $2F_o - F_c$ map, structure factors and phases based on the model were calculated with X-PLOR and analyzed by LBEST to generate weights based on the free *R*-value (Brünger, 1993; Lunin & Skovoroda, 1995; Urzhumtsev et al., 1996). Fourier maps were then generated by FFT (CCP4, 1994) using amplitudes of the form $|2wF_o - DF_c|$, where *w* and *D* are weights determined by LBEST, and phases calculated from the model. Using these maps, the model was rebuilt to better fit the electron density. Model building was done on a Silicon Graphics Indy computer using TOM (Jones, 1982). Other computations were done an Alpha computer (Digital Equipment Company).

After several rounds of rebuilding of loops between secondary structural elements and adding residues to the termini followed by refinement, the model consisted of 377 residues and had the correct sequence in place for residues 38–401 ($R_{work} = 0.25$, $R_{free} = 0.40$; 5–3.0 Å). Next, troublesome loops were rebuilt, and additions were made to the termini so that the correct sequence extended from residues 37 to 427 ($R_{work} = 0.21$, $R_{free} = 0.33$; 5–2.8 Å). Subsequently, PROCHECK (Laskowski et al., 1993) was used to determine areas of poor geometry. The poor geometry was corrected and the outer resolution was extended to 2.5 Å ($R_{work} = 0.20$, $R_{free} = 0.31$; 5–2.5 Å). To locate bound water molecules, MAPMAN (Kleywegt & Jones, 1996) was used to select peaks of height 3.5 standard deviations above the mean from a difference map, and X-PLOR was used to eliminate those peaks that were not within 3.5 Å of a protein nitrogen or oxygen atom. The graphics program O (Jones et al., 1991) was used to manually view and accept water sites. Finally, a residue was added to the N-terminus, 241 bound water molecules were added, and the resolution of refinement was extended to 2.2 Å ($R_{work} = 0.18$, $R_{free} = 0.26$; 5–2.2 Å).

The model for the allosamidin inhibitor was generated by carrying out a least-squares superposition of CiX1 and hevamine (PDB entry 1LLO) (Terwisscha van Scheltinga et al., 1995). Common secondary structural elements, namely the β-barrel, were correlated between the two proteins. The same rotation and translation matrices were used to position the allosamidin coordinates from the hevamine complex into the CiX1 space. Least-squares superpositions were done using subroutines from the graphics program TOM or O (Jones, 1982). MOLSCRIPT was used to make Figures 3 and 5 (Kraulis, 1991).

Coccidioides immitis chitinase site-directed mutagenesis

Site-directed mutagenesis was performed on active site residue Glu171. A QuikChange Site-Directed Mutagenesis Kit by Stratagene (La Jolla, California) was used to create a one base-pair change resulting in the mutation of a glutamate to a glutamine at position 171. DNA sequencing confirmed that the mutation was present and that no undesirable mutations had occurred. The E171Q mutant was purified in the same manner as the wild-type. A fluorescence assay used to show the activity of chitinase (Hollis et al., 1997) was performed using the E171Q mutant, and the results indicate that there was almost a complete loss of activity as compared to the wild-type chitinase (results not shown).

Accession number

The coordinates have been deposited with the Protein Data Bank. The ID code is 1D2K.

Acknowledgments

This work was supported by grants GM 30048 from the National Institutes of Health, grant MCB-9601096 from the National Science Foundation, and by grants from the Foundation for Research and the Welch Foundation.

References

Ampel NM. 1996. Emerging disease issues and fungal pathogens associated with HIV infection. *Emerg Infect Dis 2:*109–116.

Armand S, Tomita H, Heyraud A, Gey C, Watanabe T, Henrissat B. 1994. Stereochemical course of the hydrolysis reaction catalyzed by chitinases A1 and D from *Bacillus circulans* WL-12. *FEBS Lett 343:*177–180.

Blaiseau PL, Lafay JF. 1992. Primary structure of a chitinase-encoding gene (chi1) from the filamentous fungus *Aphanocladium album*: Similarity to bacterial chitinases. *Gene 120:*243–248.

Blake CCF, Johnson LN, Mair GA, North ACT, Phillips DC, Sarma VR. 1967. Crystallographic studies of the activity of hen egg-white lysozyme. *Proc R Soc Ser B 167*:378–388.

Brameld KA, Shrader WD, Imperiali B, Goddard WA III. 1998. Substrate assistance in the mechanism of family 18 chitinases: Theoretical studies of potential intermediates and inhibitors. *J Mol Biol 280*:913–923.

Brünger AT. 1990. Extension of molecular replacement: A new search strategy based on Patterson correlation refinement. *Acta Crystallogr A46:*46–57.

Brünger AT. 1992. *X-PLOR version 3.1: A system for X-ray crystallography and NMR.* New Haven, Connecticut: Yale University Press.

Brünger AT. 1993. Assessment of phase accuracy by cross validation: The free *R* value. *Acta Crystallogr D49:*129–147.

Bulawa CE, Osmond BC. 1990. Chitin synthase I and chitin synthase II are not required for chitin synthesis in vivo in *Saccharomyces cerevisiae*. *Proc Natl Acad Sci USA 87:*7424–7428.

CCP4 (Collaborative Computational Project Number 4). 1994. The CCP4 suite: Programs for protein crystallography. *Acta Crystallogr D50:*760–763.

Cole GT, Kirkland TN. 1991. Conidia of *Coccidioides immitis* their significance in disease initiation. In: Cole GT, Hoch HC, eds. *The fungal spore and disease initiation in plants and animals*. New York: Plenum Press. pp 403–443.

Dolan MJ, Cox RA. 1991. Production and characterization of a monoclonal antibody to the complement fixation antigen of *Coccidioides immitis. Infect Immun 59*:2175–2180.

Garcia I, Lora JM, de la Cruz J, Benitez T, Llobell A, Pintor-Toro JA. 1994. Cloning and characterization of a chitinase (chit42) cDNA from the mycoparasitic fungus *Trichoderma harzianum*. *Curr Genet 27:*83–89.

Hart PJ, Pfluger HD, Monzingo AF, Hollis T, Robertus JD. 1995. The refined crystal structure of an endochitinase from *Hordeum vulgare* L. seeds at 1.8 Å resolution. *J Mol Biol 248:*402–413.

Henrissat B, Bairoch A. 1993. New families in the classification of glycosyl hydrolases based on amino acid sequence similarities. *Biochem J 293:*781–788.

Higgins DG, Bleasby AJ, Fuchs R. 1992. CLUSTAL V: Improved software for multiple sequence alignment. *Comput Appl Biosci 8:*189–191.

Hollis T, Honda Y, Fukamizo T, Marcotte EM, Robertus JD. 1997. Kinetic analysis of barley chitinase. *Arch Biochem Biophys 336:*268–274.

Hollis T, Monzingo AF, Bortone K, Schelp E, Cox R, Robertus JD. 1998. Crystallization and preliminary X-ray analysis of a chitinase from the fungal pathogen *Coccidioides immitis*. *Acta Crystallogr D54:*1412–1413.

Johnson SM, Pappagianis D. 1992. The coccidioidal complement fixation and immunodiffusion-complement fixation antigen is a chitinase. *Infect Immun 60*:2588–2592.

Jones JDG, Grady KL, Suslow TV, Bedbrook JR. 1986. Isolation and characterization of genes encoding two chitinase enzymes from *Serratia marcescens*. *EMBO J 5:*467–473.

Jones TA. 1982. FRODO: A graphics fitting program for macromolecules. In: Sayer D, ed. *Computational crystallography*. Oxford: Clarendon Press. pp 303–317.

Jones TA, Zou JY, Cowan SW, Kjeldgaard M. 1991. Improved methods for building models in electron density maps and the location of errors in these models. *Acta Crystallogr A47*:110–119.

Kleywegt GJ, Jones TA. 1996. xdlMAPMAN and xdlDATAMAN—Programs for reformatting analysis and manipulation of biomolecular electron-density maps and reflection data sets. *Acta Crystallogr D52:*826–828.

Kraulis PJ. 1991. MOLSCRIPT: A program to produce both detailed and schematic plots of protein structure. *J Appl Crystallogr 24*:946–950.

Kuranda MJ, Robbins PW. 1991. Chitinase is required for cell separation during growth of *Saccharomyces cerevisiae*. *J Biol Chem 266:*19758–19767.

Laskowski RA, MacArthur MW, Moss DS, Thornton JM. 1993. PROCHECK: A program to check the stereochemical quality of protein structures. *J Appl Crystallogr 26:*283–291.

Lunin VY, Skovoroda TD. 1995. R-free likelihood-based estimates of errors for phases calculated from atomic models. *Acta Crystallogr A51:*880–886.

Milewski S, O'Donnell RW, Gooday GW. 1992. Chemical modification studies of the active centre of *Candida albicans* chitinase and its inhibition by allosamidin. *J Gen Microbiol 138:*2545–2550.

Minamoto GY, Rosenberg AS. 1997. Fungal infections in patients with acquired immunodeficiency syndrom. *Med Clin North Am 81:*381–409.

Monzingo AF, Marcotte EM, Hart PJ, Robertus JD. 1996. Chitinases chitosanases and lysozymes can be divided into procaryotic and eucaryotic families sharing a conserved core. *Nat Struct Biol 3:*133–140.

Nishimoto Y, Sakuda S, Takayama S, Yamada Y. 1991. Isolation and characterization of new allosamidins. *J Antibiot 44:*716–722.

Pappagianis D, Zimmer BL. 1990. Serology of coccidioidomycosis. *Clin Microbiol Rev 3*:247–268.

Perrakis A, Tews I, Dauter Z, Oppenheim AB, Chet I, Wilson KS, Vorgias CE. 1994. Crystal structure of a bacterial chitinase at 2.3 Å resolution. *Structure 2:*1169–1180.

Pishko EJ, Kirkland TN, Cole GT. 1995. Isolation and characterization of two chitinase-encoding genes (cts1 cts2) from the fungus *Coccidioides immitis*. *Gene 167:*173–177.

Terwisscha van Scheltinga AC, Armand S, Kalk KH, Isogai A, Henrissat B, Dijkstra BW. 1995. Stereochemistry of chitin hydrolysis by a plant chitinase/lysozyme and X-ray structure of a complex with allosamidin: Evidence for substrate assisted catalysis. *Biochemistry 34:*15619–5623.

Terwisscha van Scheltinga AC, Hennig M, Dijkstra BW. 1996. The 1.8 Å resolution structure of hevamine a plant chitinase/lysozyme and analysis of the conserved sequence and: structure motifs of glycosyl hydrolase family 18. *J Mol Biol 262:*243–257.

Urzhumtsev AG, Skovoroda TD, Lunin VY. 1996. A procedure compatible with X-PLOR for the calculation of electron-density maps weighted using an R-free-likelihood approach. *J Appl Crystallogr 29:*741–744.

Watanabe T, Kobori K, Miyashita K, Fujii T, Sakai H, Uchida M, Tanaka H. 1993. Identification of glutamic acid 204 and aspartic acid 200 in chitinase A1 of *Bacillus circulans* WL-12 as essential residues for chitinase activity. *J Biol Chem 268:*18567–18572.

Yang C, Zhu Y, Magee DM, Cox RA. 1996. Molecular cloning and characterization of the *Coccidioides immitis* complement fixation/chitinase antigen. *Infect Immun 64*:1992–1997.